NIH Public Access
Author Manuscript
Exp Hematol. Author manuscript; available in PMC 2011 February 1.

Published in final edited form as:
Exp Hematol. 2010 February ; 38(2): 132. doi:10.1016/j.exphem.2009.11.002.

GAS6/Mer axis regulates the homing and survival of the E2A/PBX1 positive B-cell precursor acute lymphoblastic leukemia in the bone marrow niche

Yusuke Shiozawa[1], **Elisabeth A. Pedersen**[1], and **Russell S. Taichman**[1]

[1] Department of Periodontics and Oral Medicine, University of Michigan School of Dentistry, Ann Arbor, MI

Abstract

Despite improvements in current combinational chemotherapy regimens, the prognosis of the (1;19)(q23;p13) translocation (**E2A/PBX1**) positive B-cell precursor acute lymphoblastic leukemia (**ALL**) is poor in pediatric leukemia patients. In this study, we examined the roles of GAS6/Mer axis in the interactions between E2A/PBX1 positive B-cell precursor ALL cells and the osteoblastic niche in the bone marrow. The data show that primary human osteoblasts secrete GAS6 in response to the Mer-over-expressed E2A/PBX1 positive ALL cells through MAPK signaling pathway and that leukemia cells migrate toward GAS6 using pathways activated by Mer. Importantly, GAS6 supports the survival and prevents apoptosis from chemotherapy of E2A/PBX1 positive ALL cells by inducing dormancy. Together, these data suggest that GAS6/Mer axis regulates the homing and survival of the E2A/PBX1 positive B-cell precursor ALL in the bone marrow niche.

Keywords

GAS6; Mer; osteoblasts; B-cell precursor acute lymphoblastic leukemia; E2A/PBX1

Introduction

The current 5-year event-free survival rate is nearly 80% for children with acute lymphoblastic leukemia (**ALL**) [1]. However, The (1;19)(q23;p13) translocation positive B-cell precursor ALL, a subtype of ALL accounting for 5-6% of pediatric ALL cases, is associated with a poorer prognosis [2]. The t(1;19)(q23;p13) involves the E2A gene on chromosome 19(p13.2/p13.3) and the PBX1 gene on chromosome 1(q23). The translocation results in the production of the E2A/PBX1 fusion transcript that has malignant potential [2]. Interestingly, oligonucleotide array analyses demonstrates that a B-cell leukemia subtype with a t(1;19) producing the E2A-PBX1 fusion protein significantly over expresses the receptor tryrosine kinase (**RTK**) Mer or

© 2009 International Society for Experimental Hematology. Published by Elsevier Inc. All rights reserved.

Corresponding author: Russell S. Taichman D.M.D., D.M.Sc. Department of Periodontics and Oral Medicine University of Michigan School of Dentistry, 1011 North University Avenue Ann Arbor, MI, 48109-1078, USA. Phone: 1-734-764-9952; Fax: 1-734-763-5503; rtaich@umich.edu.

Publisher's Disclaimer: This is a PDF file of an unedited manuscript that has been accepted for publication. As a service to our customers we are providing this early version of the manuscript. The manuscript will undergo copyediting, typesetting, and review of the resulting proof before it is published in its final citable form. Please note that during the production process errors may be discovered which could affect the content, and all legal disclaimers that apply to the journal pertain.

Conflict of Interest Disclosure
No financial interest/relationships with financial interest relating to the topic of this article have been declared.

NIH-PA Author Manuscript
NIH-PA Author Manuscript
NIH-PA Author Manuscript

NIH-PA Author Manuscript

NIH-PA Author Manuscript

NIH-PA Author Manuscript

MerTK [3]. In other settings, Mer expression is low to absent in normal lymphocytes [4], but is over-expressed other leukemias, including T-ALL [4] and mantle cell lymphomas [5], suggesting that Mer plays a critical role in the pathogenesis of these diseases.

Mer is a member of a RTK family that includes Axl and Sky. The Axl/Sky/Mer family is activated by a common ligand, growth arrest specific-6 (**GAS6**) [6]. GAS6 is produced by fibroblasts in the bone marrow [7] and is also present in human plasma [8-11]. Post-receptor binding events regulated by Mer are thought to establish protection from apoptosis for leukemic cells via PI3K/Akt and MAPK/Erk1/2 signaling pathways [12]. As such the anti-apoptotic pathways are thought to contribute to leukemogenesis and resistance to treatment with standard chem otherapies [12]. However, the role of GAS6/Mer in ALL, especially the E2A/PBX1 positive B-cell precursor ALL are unclear.

Adhesion molecules and secreted factors derived from bone marrow stromal cells (**BMSCs**) are known to constitute the basis of the hematopoietic stem cell (**HSC**) niche. As such BMSCs are thought to regulate HSC self-renewal, proliferation, and differentiation through the production of cytokines and intracellular signals initiated by cell-to-cell adhesion interaction [13]. BMSCs are composed of cells of mesenchymal origin known to include osteoblasts, endothelial cells, fibroblasts, and adipocytes [14]. In the early 1970's, studies examining the interaction between BMSCs and HSCs had suggested a unique and critical role for events localized at endosteal surfaces, and by inference osteoblasts, as having a central role in hematopoiesis [15,16]. Only recently however have studies demonstrated that osteoblasts comprise a crucial component of the normal [17-20] and leukemic stem cell niches [21].

In this study, it was found that GAS6 is produced in the HSC niche by osteoblasts, and that leukemia cells bearing the E2A/PBX1 fusion, expressing high levels of Mer become resistant to conventional chemotherapy in part due to quiescence induced by HSC niche-derived GAS6. Together, these data suggest that GAS6/Mer axis regulates the homing and survival of the E2A/PBX1 positive B-cell precursor ALL in the bone marrow niche. These findings suggest that the GAS6 production may serve as the basis of future relapse, and may provide an opportunity for the development of more effective chemotherapies targeting this pathway.

Materials and Methods

Cell Culture

RS 4;11 (CRL1873); SUP-B15 (ATCC 1929); and KG1a (CCL-246.1) were obtained from The American Type Culture Collection (ATCC; Rockville, MD). RCH-ACV (ACC 548); 697 (ACC 42); and Nalm6 (ACC 128) were obtained from The German Collection of Microorganisms and Cell Cultures (DSMZ; Braunschweig, Germany). The human bone marrow endothelial cells (**HBME**) were isolated from a normal Caucasian male and immortalized with SV40 large T-antigen [22]. All cell lines were cultured in RPMI 1640 (Invitrogen, Carlsbad, CA) and supplemented with 10% (v/v) fetal bovine serum (**FBS**; Invitrogen) and 1% (v/v) penicillin-streptomycin (Invitrogen), and maintained at 37°C, 5% CO_2, and 100% humidity.

Human Osteoblasts

Primary human osteoblasts were established by explant culture from normal human trabecular bone obtained from patients undergoing orthopedic surgery in accordance with the University of Michigan's Investigational Review Board, as previously described [18].

NIH-PA Author Manuscript

NIH-PA Author Manuscript

NIH-PA Author Manuscript

Generation of co-culture conditioned medium

Human osteoblasts and HBME were seeded at a concentration of 4×10^4 cells per well in 500 μl of RPMI 1640 supplemented without FBS on 24-well tissue culture plate. After 24 h, RCH-ACV cells in 100 μl of RPMI 1640 supplemented without FBS were overlaid at $0\text{-}4\times10^4$ cells per well onto the osteoblasts either directly or indirectly. At 48 h of co-culture, supernatant was collected, cleared from any free-floating cells by centrifugation for 5 min at 1000g, and then stored at -80°C.

Antibodies and Reagents

The anti-human GAS6 antibody (goat IgG); the anti-human GAS6 monoclonal antibody (clone 100127, mouse IgG2a); and the anti-human Mer monoclonal antibody (clone 125518, mouse IgG1) were purchased from R&D Systems (Minneapolis, MN). The control antibodies for these investigations included goat IgG (R&D Systems), mouse Ig G1 (clone X40) (Becton Dickinson, San Jose, CA), mouse IgG2a (clone 20102) (R&D Systems). The antibodies to phosphorylated Akt (Ser473), total Akt, phosphorylated p44/42 MAP kinase (Thr202/Tyr204), total p44/42 MAP kinase, and Dylight™ 488-conjugated goat anti-rabbit IgG (H + L) were obtained from Cell Signaling Technology (Danvers, MA). Recombinant human GAS6 was kindly provided from Amgen (Amgen; Thousand Oaks, CA). Cytosine arabinoside (**AraC**) was purchased from Sigma-Aldrich (St. Louis, MO).

RNA Extraction and Real-Time RT-PCR (*Q*RT-PCR)

*Q*RT-PCR reactions were carried out using standard techniques. Briefly, total RNA was isolated using RNeasy Mini Kit (QIAGEN, Valencia, CA), and first-strand cDNA was synthesized in a 20 μL reaction volume using 0.4 μg of total RNA. Reverse transcript products were analyzed by *Q*RT-PCR in TaqMan® Gene Expression Assays of several target genes: Axl (Hs00242357_m1), Sky (Hs00170723_m1), Mer (Hs00179024_m1), β-Actin (Hs99999903_m1) (Applied Biosystems, Foster City, CA). *Q*RT-PCR analyses were performed using 15.0 μl of TaqMan® Universal PCR Master Mix (Applied Biosystems), 1.5 μl of TaqMan® Gene Expression Assay, 1 μl of cDNA, and RNAse/DNAse-free water in a total volume of 30 μl. All sample concentrations were standardized in each reaction to exclude false-positive results. Reactions without template and/or enzyme were used as negative controls. The 2^{nd} step PCR reaction (95°C for 30 sec and 60°C for 1 min) was run for 40 cycles after an initial single cycle of 95°C for 15 min to activate the Taq polymerase. The PCR products were detected as an increase in fluorescence using an ABI PRISM 7700 instrument (Applied Biosystems). RNA quantities (C_R) were normalized to the housekeeping gene β-Actin control by using the formula $C_R=2^{(40\text{-Ct of sample})-(40\text{-Ct of control})}$. The threshold cycle (Ct) is the cycle at which a significant increase in fluorescence occurs.

Flow cytometry

Cells were stained with PE-conjugated anti-Mer antibody, or isotype matched IgG control. Flow cytometric analyses were performed in a FACS Vantage dual-laser flow cytometer (Becton Dickinson).

Cell signaling assay

Conditioned medium was obtained from RCH-ACV cells to induce cell signaling in human osteoblasts. Briefly, the cells were grown to 70% to 80% confluence in 25-cm^2 culture flask in RPMI with 10% FBS. After 48 h, the supernatant was collected, clarified by centrifugation for 5 min at 1000*g*, concentrated with Centricon YM3 filters (Millipore, Billerica, MA) and then stored at -80°C. Conditioned medium without cells serves as control. Human osteoblasts (5×10^5 cells) were incubated in RPMI medium (1 mL) without FBS for 5 h. After serum starvation, the cells were treated with 1 μg/μl of RCH-ACV conditioned medium or control

NIH-PA Author Manuscript

NIH-PA Author Manuscript

NIH-PA Author Manuscript

conditioned medium for 1 h. After 1 h incubation, the cells were fixed and permeabilized with Perm/Wash Buffer (BD Biosciences, San Jose, CA), according to manufacture's protocol. Later, the cells were stained with phosphorylated Akt, total Akt, phosphorylated p44/42 MAP kinase, and total p44/42 MAP kinase antibodies, and were subsequently stained with Dylight™ 488-conjugated secondary antibodies. Flow cytometric analyses were performed in a FACS Vantagedual-laser flow cytometer.

Cell cycling assay

Cell cycling states of RCH-ACV cells in response to GAS6 treatments were analyzed by FACS using Hoechst 33342 (Molecular Probes, Eugene, OR) and Pyronin Y (**PY**; Sigma-Aldrich) staining methods, as previously described [23]. Briefly, RCH-ACV cells (1×10^6 cells/25-cm^2 culture flask) were treated with 1 μg/ml of GAS6 or vehicle for 48 h. Thereafter, the cells were incubated in 2 μg/ml of Hoechst 33342 for 45 min and were incubated in 4 μg/mL of PY for another 45 min. Cell cycle was analyzed by flow cytometry. The cells that expressed low Hoechst 33342 and low PY, low Hoechst 33342 and high PY, and high Hoechst 33342 and high PY were determined as G0, G1, and S/G2/M state, respectively.

Immunohistochemistry

Primary human osteoblasts (5×10^5 cells/chamber) were cultured on Lab-Tek II 4-chamber slides (Nalge Nunc International, Naperville, IL). At 48 h, the cells were fixed in 4% paraformaldehyde for 25 min at room temperature, washed and endogenous peroxidase activity quenched with 75 mM NH_4Cl and 20 mM glycine in PBS at room temperature for 10 min. Thereafter, the cells were incubated with a 1:50 dilution of either the anti-human GAS6 antibody (goat IgG) or an IgG matched isotype control antibody for 1 h at room temperature. Antibody detection was performed by using a goat HRP-AEC staining kit (R&D Systems). The staining intensities of the slides were quantified with Image J software (version 1.40; National Institutes of Health (**NIH**), Bethesda, MD).

GAS6 ELISA

Antibody sandwich ELISA was used to evaluate GAS6 in human osteoblasts and HBME conditioned medium (R&D Systems). GAS6 levels were normalized to total protein in the conditioned medium.

Trans-well Invasion Assays

Cell invasion assays were performed in dual chambered 5 μM pore sized trans-well plates (BD Biosciences). RCH-ACV cells were labeled with 2.5 μg/ml of the lipophilic dye carboxyfluorescein diacetate (**CFDA**; Molecular Probes) in RPMI for 30 min at 37°C, and washed in PBS. Thereafter, the cells were left for 30 min to reduce nonspecific background, and subsequently resuspended in PBS to deliver 10^5 cells/well (100 μl of serum free RPMI) in the top chamber. Spontaneous invasion was compared to invasion supported by GAS6 (0-1 μg/ml). At the termination of the assay (4 h), the chambers were removed and fluorescence was quantified by fluorescent plate reader (Molecular Devices, Sunnyvale, CA). In some cases, 5 μg/ml of an anti-GAS6 antibody or IgG matched isotype control antibody were added into the bottom chamber, or 5 μg/ml of an anti-Mer antibody or IgG matched isotype control antibody were added into the top chamber to block the invasion of RCH-ACV cells to GAS6.

Apoptosis Assays

RCH-ACV cells (1×10^6 cells/well) were cultured in 6-well plates in RPMI medium (1 mL) without FBS for 5 h. After serum starvation, the cells were treated with 1 μg/ml GAS6 for 24 h. Thereafter, cells were stained with annexin V PE (BD Biosciences) and 7ADD (BD

NIH-PA Author Manuscript

NIH-PA Author Manuscript

NIH-PA Author Manuscript

Biosciences), according to the manufacture's protocol. Apoptotic cells were analyzed by flow cytometry.

Chemo-resistant Assays

RCH-ACV cells were plated into triplicate 96-well plates at a concentration of 5000 cells per well (100 μL per well) in growth medium with 5% FBS for 5 h. The cells were treated with GAS6 (1 μg/ml) or vehicle. After 24 h incubation, cells were treated with serial doses of AraC (0-10^{-3} M). Thereafter, the cultures were incubated in an atmosphere of 5% CO_2 and 95% O_2 at 37°C for 3 days. Cell viability was quantified by colorimetric assay using sodium 3'-[1-[(phenylamino)-carbonyl]-3,4-tetrazolium]-bis(4-methoxy-6-nitro)benzene-sulfonic acid hydrate (**XTT**; Sigma-Aldrich) and read on a multi-well scanning spectrophotometer at OD_{450} (Molecular Devices).

Statistical Analyses

All *in vitro* experiments were performed at least three times with similar results and representative assay are shown. Numerical data are expressed as mean ± standard error of the mean. Statistical analysis was performed by ANOVA or Student's *t* test using the GraphPad Instat statistical program (GraphPad Software, San Diego, CA) with significance at $P < 0.05$. For the *Q*RT-PCR assays, a Kruskal-Wallis test and Dunn's multiple comparisons tests were utilized with the level of significance set at $P < 0.05$.

Results

The leukemia cell lines express the Axl/Sky/Mer family of RTKs

Previous reports suggest that the Axl/Sky/Mer family is over-expressed in many cancers. We therefore first determined the basal expression of the Axl/Sky/Mer family in leukemia cell lines using *Q*RT-PCR (Figure 1A). Interestingly, the E2A/PBX1 positive B-cell precursor ALL cell lines RCH-ACV and 697, demonstrated significant expression of Mer compared to the others leukemia cell lines (Nalm6: t(5;12)(q33.2;p13.2) positive B-cell precursor ALL cell line; RS4;11: t(4;11)(q21;q23) positive B-cell precursor ALL cell line; SUP-B15 t(9;22)(q34;q11) positive B-cell precursor ALL cell line; and KG1a: acute myeloid leukemia (**AML**) cell line) (Figure 1A). In contrast, moderate levels of Sky and low or no Axl was expressed by the leukemic cell lines (Figure 1A). Further evaluation of the expression of the Mer at the protein level was performed by flow cytometry analysis using PE-conjugated anti-Mer antibodies. Only the E2A/PBX1 positive cell line RCH-ACV expressed significant Mer levels (Figure 1B). For these studies, RCH-ACV cells were thus chosen for further study since they expressed the high basal levels of Mer mRNA and cell surface protein (Figure 1A&B). These data suggest that the E2A/PBX1 positive B-cell precursor ALL cell lines, especially RCH-ACV cells, express the high levels of Mer.

RCH-ACV cells stimulate GAS6 production of osteoblasts

As GAS6 is the sole protein known to activate Mer, the source of GAS6 in the marrow was next explored focusing on the osteoblastic niche cells. As an initial assessment of whether GAS6 is produced by primary human osteoblasts, immunohistochemistry was performed. The data demonstrates that indeed GAS6 is produced by primary osteoblasts (Figure 2A&B). Next, to determine whether GAS6 synthesis occurs in response to leukemia cells, co-cultures of RCH-ACV cells and the primary human osteoblasts were established and conditioned medium was collected after 48 h. GAS6 levels in the supernatants were determined by ELISA. In either the co-cultures separated by porous micro-membranes (Trans-well™) or the direct cell-to-cell contact co-cultures, RCHACV cells or their conditioned medium significantly stimulated an increase in GAS6 production relative to the primary human osteoblasts alone (Figure 2C).

NIH-PA Author Manuscript

NIH-PA Author Manuscript

NIH-PA Author Manuscript

However, no GAS6 secretion or GAS6 synthesis in response to RCH-ACV cells were observed in human bone marrow endothelial cells (**HBME**), believed to participate in the HSC niche [24] (**Data not shown**). To address the mechanisms of GAS6 synthesis in human osteoblasts, human osteoblasts were treated with conditioned medium from RCH-ACV cells and cell signaling pathways were examined by FACS. Interestingly, RCH-ACV conditioned medium stimulated mostly Erk1/2 signaling pathway, while little stimulations were found in Akt signaling pathway (Table 1). These data suggest that osteoblasts express and secret GAS6, and that GAS6 synthesis occur in response to RCH-ACV cells through MAPK signaling pathway.

GAS6/Mer axis is involved in the chemotaxis of RCH-ACV cells

Next it was determined if GAS6 is chemotactic for ALL cells. For these studies chemotactic assays were performed using RCH-ACV cells. At 4 h, approximately 10-15% of the total input RCH-ACV cells migrated toward GAS6, whereas few cells migrated in its absence (Figure 3A). Inclusion of either neutralizing antibodies to GAS6 or antibodies targeting Mer itself abrogated the chemotactic effect of GAS6 (Figure 3B). These data suggested that the migration of ALL cells to GAS6 is dependent on Mer.

GAS6 inhibits apoptosis of RCH-ACV cells and protects RCH-ACV cells from chemotherapy

To determine if GAS6 regulates apoptosis, RCH-ACV cells were starved in serum free medium containing either GAS6 (1 μg/ml) or vehicle. After 12 h, apoptotic cells were detected by flow cytometry analysis by evaluating annexin V staining. Fewer apoptotic cells were detected in the GAS6 treated cells than vehicle treatment (Figure 4A).

As GAS6 protects RCH-ACV cells from apoptosis induced by serum withdrawl, it was determined if GAS6 protects RCH-ACV cells from chemotherapy. For these studies the viability of RCH-ACV following treatment with AraC was evaluated using an XTT assay. RCH-ACV incubated with GAS6 showed higher viability following AraC treatment than without GAS6 (Figure 4B). Next, the cell cycle state of GAS6-treated RCH-ACV cells and vehicle-treated RCH-ACV cells were compared, since most of conventional chemotherapeutic agents target cells that are actively dividing. As expected, GAS6 fascinated G0 arrest of RCH-ACV cells (Table 2). These data suggest that GAS6 prevents the apoptosis of RCH-ACV cells, and that RCH-ACV cells acquire resistance to chemotherapy thorough GAS6/Mer pathway by inducing dormancy in RCH-ACV cells.

Discussions

In this study, the GAS6/Mer pathway was explored as a basis for interactions between E2A/PBX1 positive B-cell precursor acute lymphoblastic leukemia cells and the osteoblastic niche in the bone marrow. We found that the primary human osteoblasts secrete GAS6 in response to the E2A/PBX1 positive leukemia cells, and that leukemia cells migrate toward GAS6 using Mer. Importantly, expression of Mer in E2A/PBX1 positive leukemia appears to confer drug resistance, suggesting that GAS6/Mer interactions may be the basis of leukemic relapse in this leukemia. Together, these data suggest that GAS6/Mer axis regulates the homing and survival of the E2A/PBX1 positive B-cell precursor acute lymphoblastic leukemia in the bone marrow niche.

The bone marrow is not only the primary site of most leukemias, but also one of the principle site of leukemic relapse. *In vitro* and *in vivo* studies suggest that BMSCs promote the growth, survival, and drug-resistance of hematopoietic malignancies [25-27]. Direct cell-to-cell contact between leukemia and BMSCs is thought to contribute significantly to drug resistance. For example, the adhesion of B-lineage ALL to BMSCs provides protection from cytarabine and etposide-induced apoptosis through VLA-4/VCAM-1 interactions [28]. Similarly, VLA-4/

NIH-PA Author Manuscript

NIH-PA Author Manuscript

NIH-PA Author Manuscript

fibronectin interactions also facilitate the induction of drug resistances by AML cells through PI-3K/Akt signaling, where antibody to VLA-4 alleviates the drug resistance [29]. As a consequence interactions with BMSCs may contribute to growth arrest/quiescence, the induction of resistance of leukemic cells to most current chemotherapy that targets proliferating cells.

It has been widely reported that GAS6 alte rs proliferation and survival of several different types of cancer cells [30-34]. The current study demonstrates that GAS6 protects the E2A/PBX1 positive leukemia cells from the induction of apoptotic cell death and chemotherapy by inducing dormancy. In somewhat parallel studies, we have recently shown that GAS6 inhibits proliferation, supported survival, prevented apoptosis from chemotherapy and regulated cell-cycling in prostate cancer (submitted). Where GAS6 inhibits proliferation of prostate cancers that express high levels of Mer by producing IL-8 through the mitogen-activated protein kinase (MEK)/ERK/Jun/Fos pathway [34]. Interestingly, GAS6 expressed by stromal cells also reduces cell-cycling state of HSCs [7]. While further studies are needed, GAS6 may serve as a common inflection point regulating both stem cell quiescence and tumor dormancy. Recently Linger RM, et al. demonstrated that when Mer expression is inhibited in Mer over-expressing E2A/PBX1 positive leukemia cells, the cells loose chemo-resistance to 6-MP and VP-16 by reducing phosphorylated Erk1/2 and mammalian target of rapamycin (**mTOR**) signaling pathways [35]. These findings suggest that GAS6/Mer axis plays an important role in chemo-resistance of Mer positive leukemias or cancers.

Recent studies have demonstrated that osteoblasts play an important role in the HSC niche [17-20]. The HSC niche is thought to regulate HSC self-renewal, proliferation, and differentiation through production of cytokines and cellular signals that are initiated by cell-to-cell adhesive interactions between HSCs and the components of the HSC niche.

Where the osteoblastic niche is thought to induce dormancy of HSCs [36]. More recently, it has also demonstrated that osteoblasts comprise a crucial component of the leukemic stem cell niches [21]. Although there are limitations, our present data may also support that osteoblasts serve as the leukemic stem cell niche in the marrow. Since it has been appreciated a concept that a variety of the tumors parasitize the HSC niche [37], leukemia cells may also target the HSC niche when they home to the bone marrow. If leukemia cells occupy the same niche as HSCs themselves, then it is likely that the initial role of the HSC niche will be to induce dormancy in leukemia cells. Future studies will be needed to gain a more complete understanding of the molecular events activated by leukemic cell-niche interactions. These studies may provide crucial clues as to how to direct chemotherapy to prevent leukemic relapse of E2A/PBX1 positive B-cell precursor ALL and other Mer positive cancers.

Acknowledgments

We thank Amgen for providing us recombinant human GAS6. We also thank Drs. Laurie K. McCauley and Evan T. Keller for scientific discussions. We also thank the Pediatric Oncology Research Fellowship (Y.S.), the National Cancer Institute (R.S.T.), the Department of Defense (R.S.T.), and the Prostate Cancer Foundation (R.S.T.).

Reference Lists

1. Pui CH, Relling MV, Downing JR. Acute lymphoblastic leukemia. N Engl J Med 2004;350:1535–1548. [PubMed: 15071128]
2. Piccaluga PP, Malagola M, Rondoni M, et al. Poor outcome of adult acute lymphoblastic leukemia patients carrying the (1;19)(q23;p13) translocation. Leuk Lymphoma 2006;47:469–472. [PubMed: 16396770]

NIH-PA Author Manuscript

NIH-PA Author Manuscript

NIH-PA Author Manuscript

3. Yeoh EJ, Ross ME, Shurtleff SA, et al. Classification, subtype discovery, and prediction of outcome in pediatric acute lymphoblastic leukemia by gene expression profiling. Cancer Cell 2002;1:133–143. [PubMed: 12086872]
4. Graham DK, Salzberg DB, Kurtzberg J, et al. Ectopic expression of the protooncogene Mer in pediatric T-cell acute lymphoblastic leukemia. Clin Cancer Res 2006;12:2662–2669. [PubMed: 16675557]
5. Ek S, Hogerkorp CM, Dictor M, Ehinger M, Borrebaeck CA. Mantle cell lymphomas express a distinct genetic signature affecting lymphocyte trafficking and growth regulation as compared with subpopulations of normal human B cells. Cancer Res 2002;62:4398–4405. [PubMed: 12154046]
6. Chen J, Carey K, Godowski PJ. Identification of Gas6 as a ligand for Mer, a neural cell adhesion molecule related receptor tyrosine kinase implicated in cellular transformation. Oncogene 1997;14:2033–2039. [PubMed: 9160883]
7. Dormady SP, Zhang XM, Basch RS. Hematopoietic progenitor cells grow on 3T3 fibroblast monolayers that overexpress growth arrest-specific gene-6 (GAS6). Proc Natl Acad Sci U S A 2000;97:12260–12265. [PubMed: 11050245]
8. Clauser S, Bachelot-Lozat C, Fontana P, et al. Physiological plasma Gas6 levels do not influence platelet aggregation. Arterioscler Thromb Vasc Biol 2006;26:e22. [PubMed: 16484600]
9. Balogh I, Hafizi S, Stenhoff J, Hansson K, Dahlback B. Analysis of Gas6 in human platelets and plasma. Arterioscler Thromb Vasc Biol 2005;25:1280–1286. [PubMed: 15790929]
10. Burnier L, Borgel D, Angelillo-Scherrer A, Fontana P. Plasma levels of the growth arrest-specific gene 6 product (Gas6) and antiplatelet drug responsiveness in healthy subjects. J Thromb Haemost 2006;4:2283–2284. [PubMed: 16999853]
11. Borgel D, Clauser S, Bornstain C, et al. Elevated growth-arrest-specific protein 6 plasma levels in patients with severe sepsis. Crit Care Med 2006;34:219–222. [PubMed: 16374177]
12. Keating AK, Salzberg DB, Sather S, et al. Lymphoblastic leukemia/lymphoma in mice overexpressing the Mer (MerTK) receptor tyrosine kinase. Oncogene 2006;25:6092–6100. [PubMed: 16652142]
13. Miura Y, Gao Z, Miura M, et al. Mesenchymal stem cell-organized bone marrow elements: an alternative hematopoietic progenitor resource. Stem Cells 2006;24:2428–2436. [PubMed: 17071859]
14. Taichman RS. Blood and bone: two tissues whose fates are intertwined to create the hematopoietic stem-cell niche. Blood 2005;105:2631–2639. [PubMed: 15585658]
15. Patt HM, Maloney MA. Bone formation and resorption as a requirement for marrow development. Proc Soc Exp Biol Med 1972;140:205–207. [PubMed: 4555913]
16. Lord BI, Hendry JH. The distribution of haemopoietic colony-forming units in the mouse femur, and its modification by x rays. Br J Radiol 1972;45:110–115. [PubMed: 4550739]
17. Calvi LM, Adams GB, Weibrecht KW, et al. Osteoblastic cells regulate the haematopoietic stem cell niche. Nature 2003;425:841–846. [PubMed: 14574413]
18. Taichman RS, Emerson SG. Human osteoblasts support hematopoiesis through the production of granulocyte colony-stimulating factor. J Exp Med 1994;179:1677–1682. [PubMed: 7513014]
19. Zhang J, Niu C, Ye L, et al. Identification of the haematopoietic stem cell niche and control of the niche size. Nature 2003;425:836–841. [PubMed: 14574412]
20. Arai F, Hirao A, Ohmura M, et al. Tie2/angiopoietin-1 signaling regulates hematopoietic stem cell quiescence in the bone marrow niche. Cell 2004;118:149–161. [PubMed: 15260986]
21. Ninomiya M, Abe A, Katsumi A, et al. Homing, proliferation and survival sites of human leukemia cells in vivo in immunodeficient mice. Leukemia 2007;21:136–142. [PubMed: 17039228]
22. Lehr JE, Pienta KJ. Preferential adhesion of prostate cancer cells to a human bone marrow endothelial cell line. J Natl Cancer Inst 1998;90:118–123. [PubMed: 9450571]
23. Gothot A, Pyatt R, McMahel J, Rice S, Srour EF. Functional heterogeneity of human CD34(+) cells isolated in subcompartments of the G0 /G1 phase of the cell cycle. Blood 1997;90:4384–4393. [PubMed: 9373249]
24. Kiel MJ, Yilmaz OH, Iwashita T, Terhorst C, Morrison SJ. SLAM family receptors distinguish hematopoietic stem and progenitor cells and reveal endothelial niches for stem cells. Cell 2005;121:1109–1121. [PubMed: 15989959]
25. Bewick MA, Lafrenie RM. Adhesion dependent signalling in the tumour microenvironment: the future of drug targetting. Curr Pharm Des 2006;12:2833–2848. [PubMed: 16918414]

NIH-PA Author Manuscript

NIH-PA Author Manuscript

NIH-PA Author Manuscript

26. Li ZW, Dalton WS. Tumor microenvironment and drug resistance in hematologic malignancies. Blood Rev 2006;20:333–342. [PubMed: 16920238]
27. Ramasamy R, Lam EW, Soeiro I, Tisato V, Bonnet D, Dazzi F. Mesenchymal stem cells inhibit proliferation and apoptosis of tumor cells: impact on in vivo tumor growth. Leukemia 2007;21:304–310. [PubMed: 17170725]
28. Mudry RE, Fortney JE, York T, Hall BM, Gibson LF. Stromal cells regulate survival of B-lineage leukemic cells during chemotherapy. Blood 2000;96:1926–1932. [PubMed: 10961896]
29. Matsunaga T, Takemoto N, Sato T, et al. Interaction between leukemic-cell VLA-4 and stromal fibronectin is a decisive factor for minimal residual disease of acute myelogenous leukemia. Nat Med 2003;9:1158–1165. [PubMed: 12897778]
30. Holland SJ, Powell MJ, Franci C, et al. Multiple roles for the receptor tyrosine kinase axl in tumor formation. Cancer Res 2005;65:9294–9303. [PubMed: 16230391]
31. Budagian V, Bulanova E, Orinska Z, et al. Soluble Axl is generated by ADAM10-dependent cleavage and associates with Gas6 in mouse serum. Mol Cell Biol 2005;25:9324–9339. [PubMed: 16227584]
32. van Ginkel PR, Gee RL, Shearer RL, et al. Expression of the receptor tyrosine kinase Axl promotes ocular melanoma cell survival. Cancer Res 2004;64:128–134. [PubMed: 14729616]
33. Sainaghi PP, Castello L, Bergamasco L, Galletti M, Bellosta P, Avanzi GC. Gas6 induces proliferation in prostate carcinoma cell lines expressing the Axl receptor. J Cell Physiol 2005;204:36–44. [PubMed: 15605394]
34. Wu YM, Robinson DR, Kung HJ. Signal pathways in up-regulation of chemokines by tyrosine kinase MER/NYK in prostate cancer cells. Cancer Res 2004;64:7311–7320. [PubMed: 15492251]
35. Linger RM, Deryckere D, Brandao L, et al. Mer receptor tyrosine kinase is a novel therapeutic target in pediatric B-cell acute lymphoblastic leukemia. Blood. 2009
36. Yin T, Li L. The stem cell niches in bone. J Clin Invest 2006;116:1195–1201. [PubMed: 16670760]
37. Shiozawa Y, Havens AM, Pienta KJ, Taichman RS. The bone marrow niche: habitat to hematopoietic and mesenchymal stem cells, and unwitting host to molecular parasites. Leukemia 2008;22:941–950. [PubMed: 18305549]

NIH-PA Author Manuscript
NIH-PA Author Manuscript
NIH-PA Author Manuscript

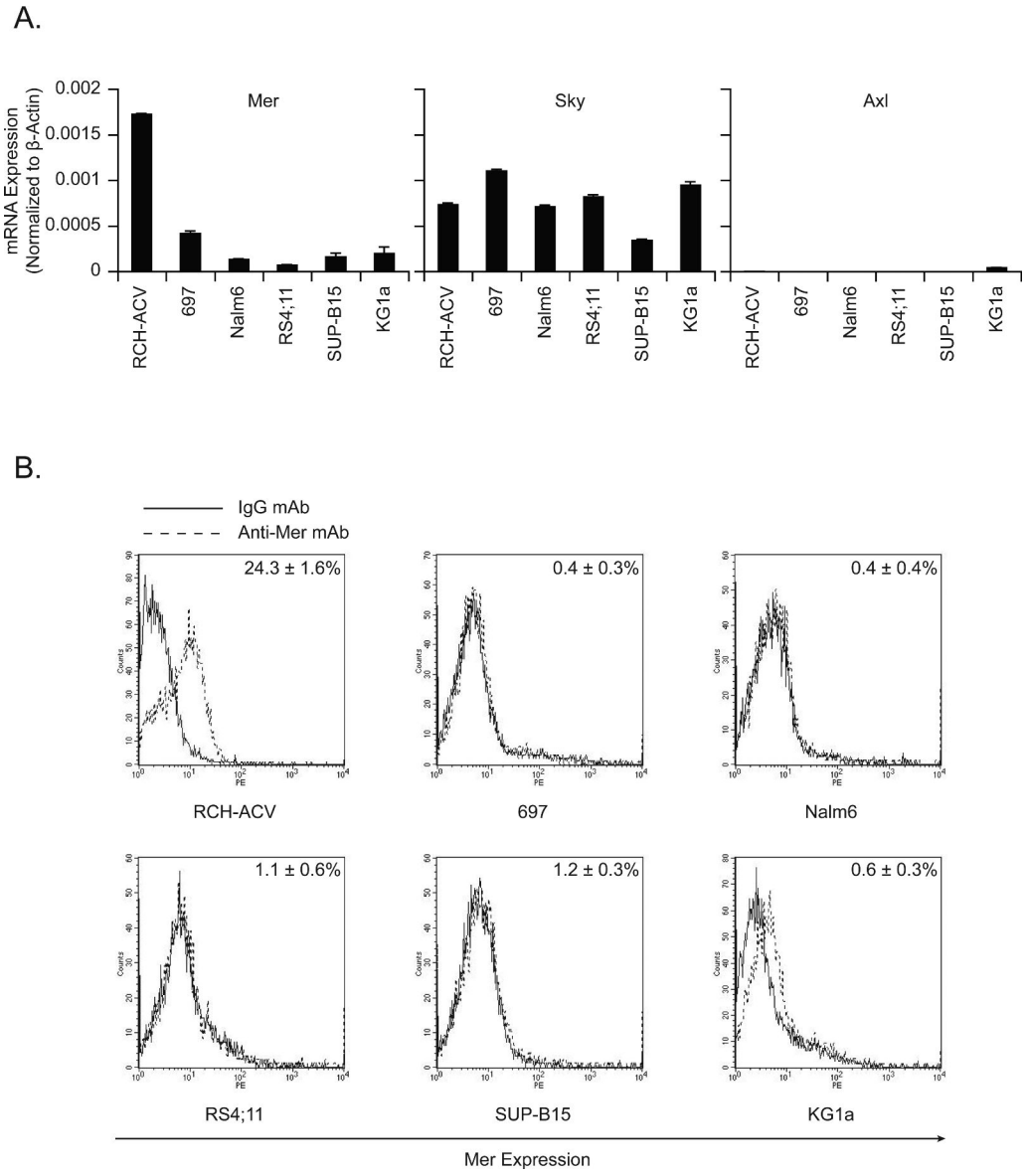

Figure 1. Expression of GAS6 receptors in human leukmia cell lines

(**A**) Expression of GAS6 receptor (Axl, Sky, Mer) mRNA in human leukemic cell lines as detected by real-time RT-PCR. (**B**) Mer protein levels expressed by human leukemic cells analyzed by flow cytometry. Cells were labeled with isotype-matched IgG control (solid line) or anti-Mer monoclonal antibodies (dotted line) before analysis. Data are presented the mean ± standard error of the mean and are representative of at least three independent experiments.

NIH-PA Author Manuscript
NIH-PA Author Manuscript
NIH-PA Author Manuscript

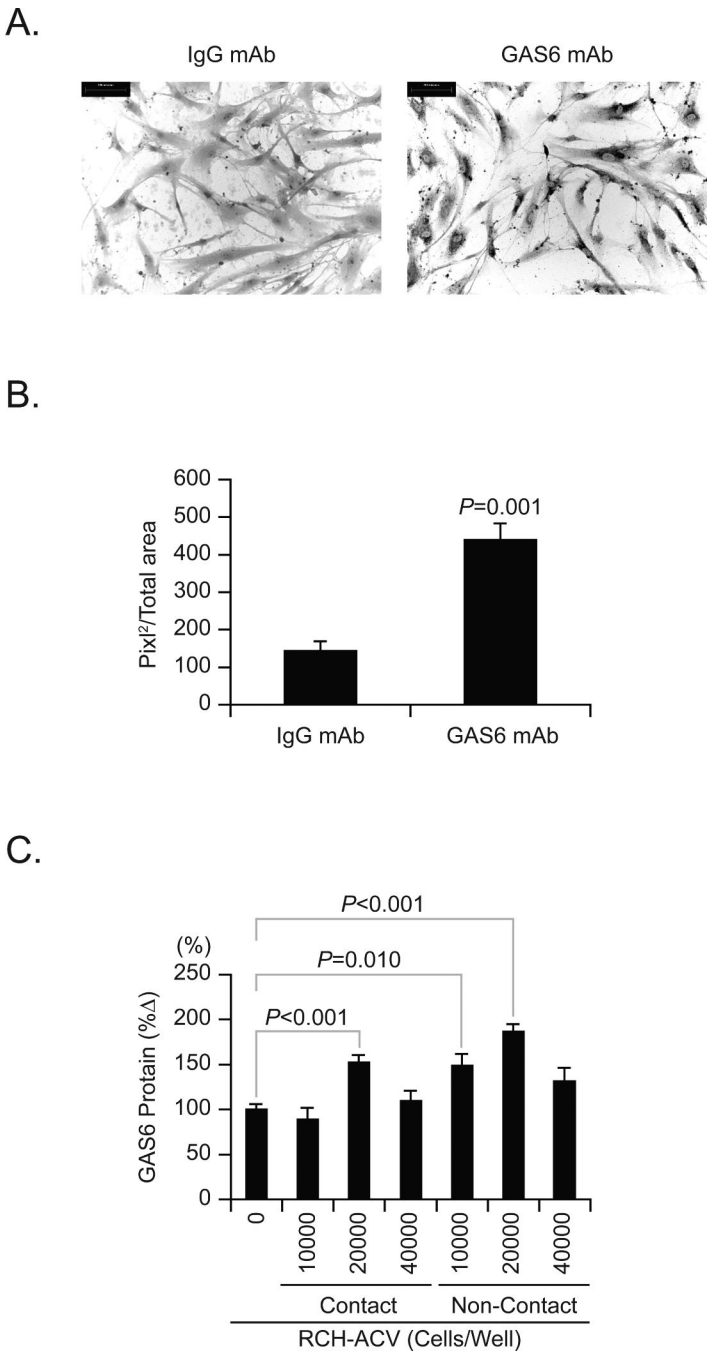

Figure 2. Expression of GAS6 by human osteoblasts

(**A**) Immunohistochemistry for GAS6 was performed on the primary human osteoblasts using monoclonal antibodies or isotype-matched IgG controls. (**B**) Quantitative digital image analyses of (A). Data are presented as the mean ± standard error of the mean. *Represents significant different from isotype-matched controls ($P<0.05$). (**C**) RCH-ACV cells (0-40000 cells) were seeded directly or indirectly onto 40000 primary human osteoblast monolayers in 24-well tissue culture plates in serum free condition. At 48 h, conditioned medium was collected and GAS6 protein levels were analyzed by ELISA. Data from a representative of three experiments are presented as the mean ± standard error of the mean. *Represents significant different from the primary human osteoblasts alone ($P<0.05$).

NIH-PA Author Manuscript
NIH-PA Author Manuscript
NIH-PA Author Manuscript

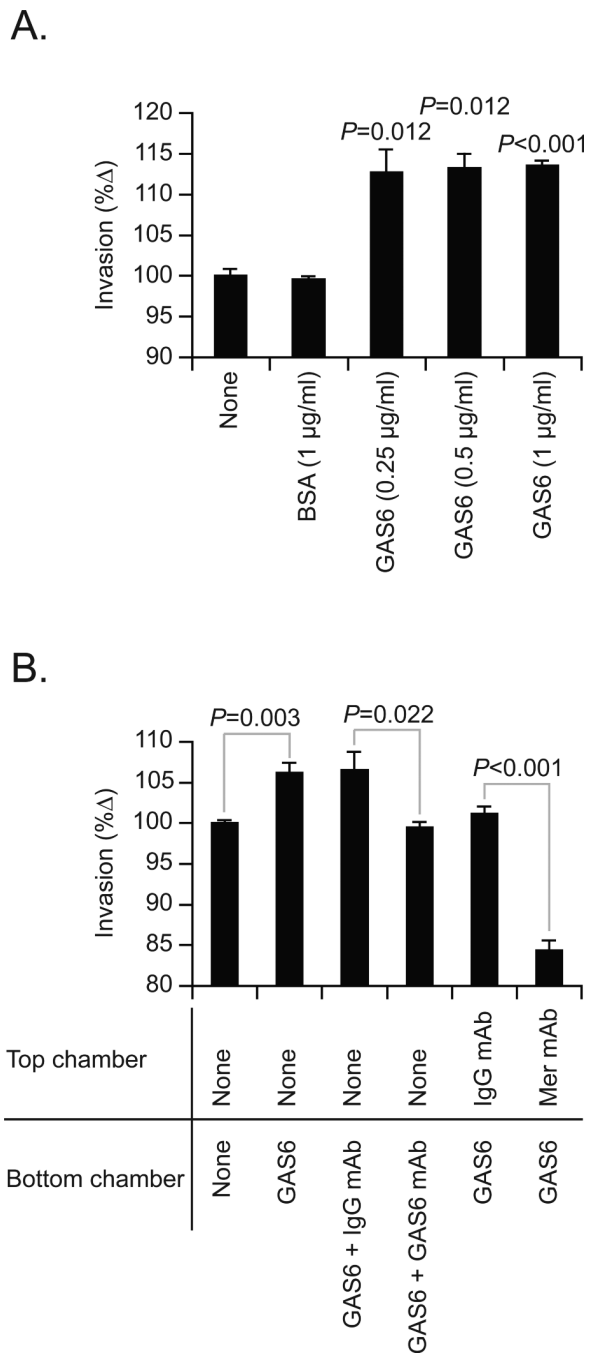

Figure 3. GAS6/Mer axis regulates the migration of RCH-ACV cells

(**A**) Transwell™ migration assays were performed to determine if GAS6 (0-1 μg/ml) serves as a chemoattractant for RCH-ACV cells. Data are presented as mean ± standard error of the mean from triplicate determinations. BSA was served as negative control. *Represents significant different from spontaneous invasion ($P<0.05$). (**B**) Chemotaxis of RCH-ACV cells in response to GAS6 were analyzed in the presence or absence of antibodies that blocked the function of GAS6 or isotype-matched controls for 30 min at 4°C. RCH-ACV cells were also treated with either blocking anti-Mer antibody or isotype-matched control for 30 min at 4°C. After washing to remove excess antibodies, RCH-ACV cells were placed in the upper wells and allowed to migrate for 4 h. Data are presented as the mean ± standard error of the mean

and as the percentage of migrated cells. *Represents significant difference from controls (spontaneous invasion or IgG control) ($P<0.05$).

NIH-PA Author Manuscript
NIH-PA Author Manuscript
NIH-PA Author Manuscript

NIH-PA Author Manuscript
NIH-PA Author Manuscript
NIH-PA Author Manuscript

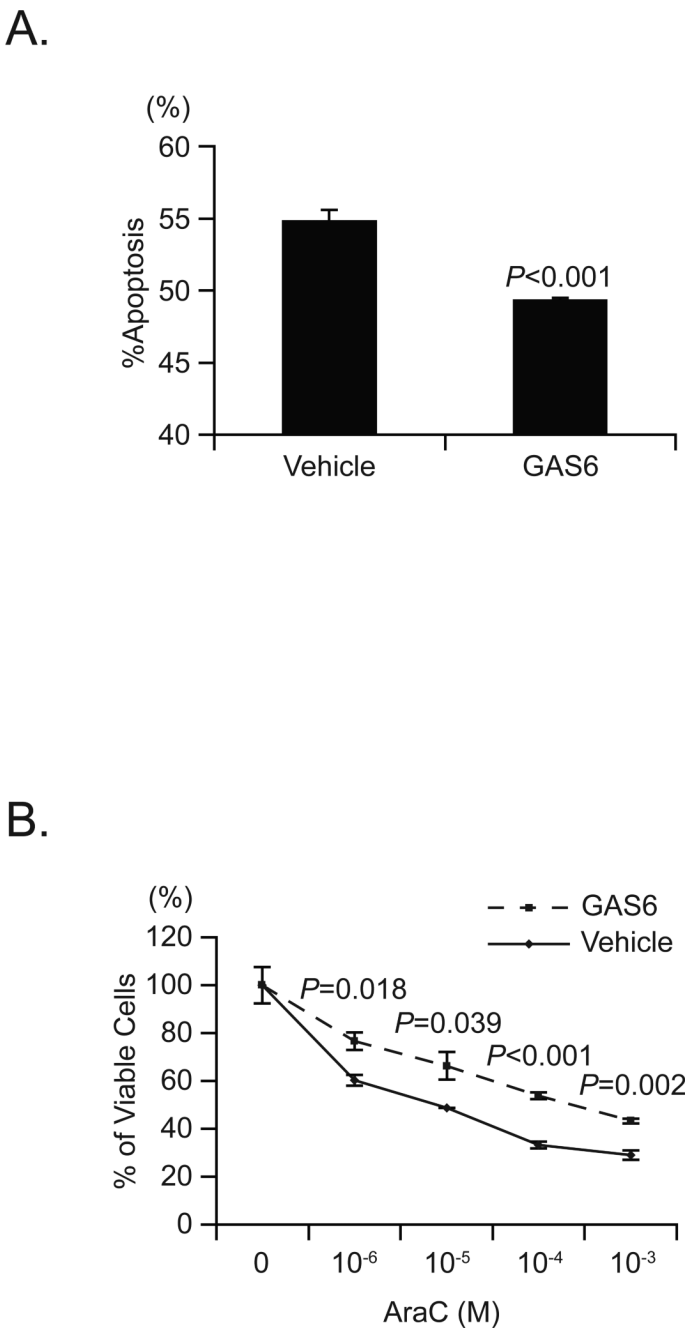

Figure 4. GAS6 inhibits apoptosis of RCH-ACV cells and prevents RCH-ACV cells from chemotherapy

(**A**) The effects of GAS6 on apoptosis of RCH-ACV cells were measured by annexin V staining. RCH-ACV cells were treated with GAS6 (1 μg/ml) or vehicle in the serum free media for 12 h. The percentage of apoptotic cells was assessed by flow cytometry. Data are presented as the mean ± standard error of the mean from three independent experiments. *Represents significant difference from vehicle treatments ($P<0.05$). (**B**) After 24 h incubation with GAS6 (1 μg/ml) or vehicle in 5% FBS condition, RCH-ACV cells were treated with AraC (0-10^{-3} M). At 48 h incubation, percentage of viable cells was assessed by XTT assay. Data are presented as the mean ± standard error of the mean from three independent experiments. *Represents significant difference from vehicle treatments ($P<0.05$).

NIH-PA Author Manuscript
NIH-PA Author Manuscript
NIH-PA Author Manuscript

Table 1

The effects of RCH-ACV CM treatment on the cell signaling pathways of human osteoblasts

	Cell Signaling Pathway					
CM	**Akt (%)**	**P-Akt (%)**	**P-Akt/Akt**	**Erk1/2 (%)**	**P-Erk1/2 (%)**	**P-Erk1/2/Erk1/2**
Control	34.0 ± 1.0	27.7 ± 0.8	0.81 ± 0.02	59.5 ± 1.7	39.3 ± 1.1	0.66 ± 0.02
RCH-ACV	33.8 ± 1.0	31.5 ± 1.0	0.93 ± 0.03	58.0 ± 1.7	47.1 ± 1.4	0.81 ± 0.02
P value			0.031			0.007

Human osteoblasts were exposed RCH-ACV CM (1 μg/μl) or control CM for 1 h. Cell signaling pathways in human osteoblasts were assessed by flow cytometry. Data are presented as mean ± standard error of the mean from triplicate determinations. Significant different from control CM treatment. CM: conditioned medium. P: phosphorylated.

Exp Hematol. Author manuscript; available in PMC 2011 February 1.

NIH-PA Author Manuscript

NIH-PA Author Manuscript

NIH-PA Author Manuscript

Table 2

The effects of GAS6 on the cell-cycling state of RCH-ACV

	%Cell		
Cell Cycle	**Vehicle**	**GAS6**	**P value**
G0	56.6 ± 2.5	65.8 ± 2.4	0.028
G1	17.6 ± 2.1	11.6 ± 1.2	0.040
S/G2/M	25.8 ± 1.0	22.6 ± 1.5	0.123

RCH-ACV were treated with GAS6 (1 μg/ml) for 48 h. Cell-cycling states of RCH-ACV were assessed by flow cytometry. Data are presented as mean ± standard error of the mean from triplicate determinations. Significantly different from vehicle treatment.